Control of Valence-Band Hole Spin by Electric Field

A. Dargys*

Semiconductor Physics Institute
A. Goštauto 11, 2600 Vilnius, Lithuania

(Received November 28, 2003)

Coherent properties of the hole spin in an electric field are investigated. The tunneling between valence bands is used to control the transitions between the spin states. Extensive numerical studies using the time-dependent Schrödinger equation for valence band are presented to demonstrate the characteristic properties of the hole spin dynamics in dc, harmonic, as well as optimized electric fields for real valence bands of silicon. The paper also shows how one can connect the average hole spin with the initial hole wave function in the time-dependent Schrödinger equation.

PACS numbers: 72.20.Jv, 73.40.Gk, 78.55.–m, 79.90.+b

1. Introduction

An important ingredient in the fast developing field of spintronics, where both the electronic charge and spin are on equal footing in the device operation, is the possibility to control the spin states of a ballistically moving or drifting charge carrier [1]. Normally, the control is done by a constant or time-varying magnetic field. The best known example of such quantum control is evidenced by the nuclear magnetic resonance which has found a wide application in chemical and medical tomography [2]. However, contrary to electric field, the magnetic field is "inert", thus, it appears difficult to achieve fast spin switching between magnetic eigenstates of the quantum system if picosecond or shorter duration magnetic field pulses are used. To have an access to magnetic degrees of freedom by electric field, one usually resorts to the relativistic interaction — better known as spin–orbit interaction — between the electric field and the electron magnetic moment. In atomic physics, the use of spin polarized electronic beams has proved to be very effective in the investigations of spin–orbit effects in the electron–atom collisions [3, 4].

*e-mail: dargys@pfi.lt

As concerns energy-band spins in semiconductors, the main investigations, apart from interband optical spectroscopy in the magnetic field, were focused on the optical orientation, where overgap photoluminescence was used to study the conduction-band spin properties in bulk semiconductors [5]. After the proposal of the spin field effect transistor (spin-FET) by Datta and Das [6] in the last decade, a new stimulus in the investigation of spin-polarized transport in semiconductors resurged. Recently, the spin-FET that is supposed to work in the diffusive regime rather than in the ballistic regime was proposed [7]. The crucial ingredient, which makes the control of electron spin possible in 2D structures, is the spin–orbit interaction at the interface of two semiconductors (the Rashba interaction), the strength of which can be controlled by electric field applied to the gate electrode.

As concerns the valence bands of semiconductors, the spin–orbit interaction here is strong enough even in bulk semiconductors, where valence band branches correspond to different values of the total angular momentum. For example, in elementary and A_3B_5 semiconductors the projection of the total angular momentum for heavy-mass band holes is predominantly equal to $\pm\frac{3}{2}$, while for light-mass band it is $\pm\frac{1}{2}$. Application of an external electric field mixes various valence band branches, most strongly at the center of the Brillouin zone, as a result the hole tunneling between various branches may take place [8–10]. If intervalence band scattering by phonons prevails, the mixing of the valence bands by electric field usually is neglected [11]. However, under intense ultrashort pulse excitation of the p-type semiconductor there may be a substantial contribution of the tunneling to intervalence transitions [12, 13]. Recently, it was shown that the tunneling mixing of valence bands by electric field can also be used to control hole spin [14]. In Ref. [14] the simplest case of two parabolic and spherical bands was considered, where it was shown that the band mixing in electric fields in principle could be used to switch the hole spin coherently between two spin states by femtosecond pulses that are shorter than the lattice-limited dephasing time of the hole wave function.

In this paper a more realistic situation is analyzed, where all three nonspherical and warped valence bands — heavy-mass, light-mass, and spin–orbit split-off — are included. Since under short pulse excitation the initial conditions play very important role, in the next section at first we shall stop on the initial conditions that are related to valence band hole spin. In the next two sections, numerical results that illustrate hole spin properties at short times in dc, harmonic, and optimized electric fields are presented.

2. Initial conditions and equations solved

As known, the valence band of tetrahedral semiconductors consists of the heavy- and light-mass bands which merge at the wave vector $\boldsymbol{k} = \mathbf{0}$ and of the split-off band separated by energy Δ. At $\boldsymbol{k} = \mathbf{0}$, the spin is a good quantum number (in a sense that the hole spin operator commutes with the Hamiltonian). The

total angular momentum, which for simplicity here will be referred to as spin, for heavy- and light-mass bands is $J = \frac{3}{2}$ (in units of $\hbar$). The spinor $|J = \frac{3}{2}, m = \pm\frac{3}{2}\rangle$, where m is the magnetic quantum number, corresponds to heavy-mass and $|J = \frac{3}{2}, m = \pm\frac{1}{2}\rangle$ corresponds to light-mass band. The spinor $|J = \frac{1}{2}, m = \pm\frac{1}{2}\rangle$ describes the spin–orbit split-off band. As mentioned, J and m could be used to identify the hole wave function at $\boldsymbol{k} = \mathbf{0}$ or in the vicinity of this point. However, for distant points, due to mixing of the spinors, such approximation is unsatisfactory, a J and m are no longer good quantum numbers. To have a quantitative measure of the influence of mixing of the basis functions at points where $\boldsymbol{k} \neq \mathbf{0}$, in Fig. 1 there is plotted the dependence of the square of hole spin $\langle \boldsymbol{J}^2 \rangle = \langle J, m | J_x^2 + J_y^2 + J_z^2 | J, m \rangle$, where J_x, J_y, and J_z are the Cartesian components of the spin operator $\boldsymbol{J}$. The calculations were performed for realistic bands of silicon. The following Luttinger–Kohn parameters were used: $\gamma_1 = 4.22$, $\gamma_2 = 0.53$, $\gamma_3 = 1.38$, $\Delta = 0.0426$ eV. The method of calculation is described in [15]. At $\boldsymbol{k} = \mathbf{0}$, one has $\langle \boldsymbol{J}^2 \rangle_{\mathrm{h,l}} = \frac{15}{4}$ for both heavy- and light-mass bands, while for the split-off band one has $\langle \boldsymbol{J}^2 \rangle_{\mathrm{s}} = \frac{3}{4}$. These values coincide with those in the atomic physics: $\langle \boldsymbol{J}^2 \rangle = J(J+1)$. At finite values of $\boldsymbol{k}$, as seen from Fig. 1, the strongest mixing takes place between light-mass and split-off bands. The mixing is anisotropic: the smallest mixing is in the $\langle 100 \rangle$-type while the strongest one is the $\langle 111 \rangle$-type directions. The wave vector $k = 0.23$ nm^{-1} in the latter case gives the hole energies 8.58, 27.7, and 80.6 meV, respectively, for heavy-, light-, and split-off bands. From Fig. 1 one can also see that $\langle \boldsymbol{J}^2 \rangle_{\mathrm{h}}$ is nearly independent of $\boldsymbol{k}$. However, this is not a general property. For example, its value drops down to 2.7 at $|\boldsymbol{k}| = 0.5$ nm^{-1}, when $\boldsymbol{k} \parallel \langle 110 \rangle$.

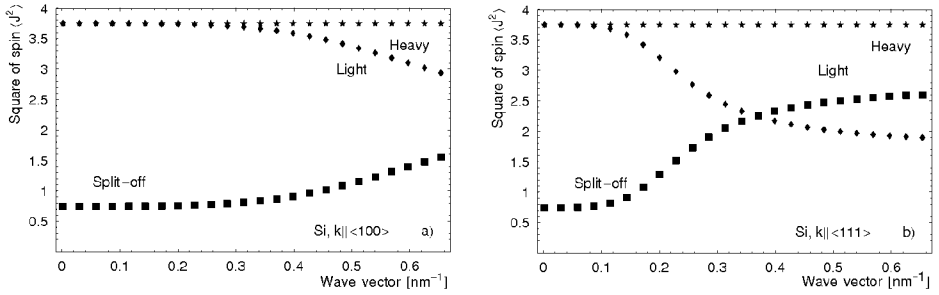

Fig. 1. Dependence of the square of hole spin on the magnitude of hole wave vector $\boldsymbol{k}$ for heavy-mass, light-mass, and split-off bands. (a) $\boldsymbol{k} \parallel \langle 100 \rangle$, (b) $\boldsymbol{k} \parallel \langle 111 \rangle$.

From what has been said it is clear that, apart from uninteresting case $\boldsymbol{k} = \mathbf{0}$, the hole spin quantum numbers are unsuitable for the description of the initial conditions in the time-dependent Schrödinger equation. This property reflects the fact that the valence band Hamiltonian and the spin operator do not commute and, therefore, the hole cannot possess a well defined energy and spin at the same time.

In the numerical simulations described in next two sections we shall assume that at moments $t < 0$, before switching of the electric field, in the semiconductor there are ballistic holes characterized by $\boldsymbol{k}$ and a well defined band energy $\varepsilon_i(\boldsymbol{k})$, where i is the band index. Since the density of states in the heavy-mass band is much larger than that in the light-mass band, in the simulation we shall also assume that the ballistic holes at $t = 0$ occupy the heavy-mass band only. The hole spin at $t = 0$ will be characterized by average (in a quantum mechanical sense) spin value $\langle \boldsymbol{J} \rangle = \langle \psi_i | \boldsymbol{J} | \psi_i \rangle$, where ψ_i is the wave function of the i-th band. Therefore, we assume that the direction and only an average value of the spin is defined by a spin injector, for example, by electrical contact fabricated from the ferromagnetic semiconductor [16]. A limit of negligible concentration of the injected holes will be considered.

In Ref. [15] it was shown that the average hole spin can be described by two parameters, a and ϕ, if the hole is in one of the bands. Specifically, if at $t = 0$ the hole is in the heavy-mass band — the case we are interested here in — then its initial wave function in the energy representation can be described by the following superposition state:

$$f = (a, \mathrm{e}^{\mathrm{i}\phi}\sqrt{1-a^2}, 0, 0, 0, 0). \tag{1}$$

The following order of bands is assumed ($f_{\mathrm{h}}^{(+)}$, $f_{\mathrm{h}}^{(-)}$, $f_{\mathrm{l}}^{(+)}$, $f_{\mathrm{l}}^{(-)}$, $f_{\mathrm{s}}^{(+)}$, $f_{\mathrm{s}}^{(-)}$), where the subscripts h, l, and s denote heavy-, light-, and split-off bands and the superscripts (+) and (−) correspond to two degenerate states. The wave function (1) is normalized to unity. Similar superposition states can be written for other two bands. In Table the relations between average values of the spin components $\{\langle J_x \rangle, \langle J_y \rangle, \langle J_z \rangle\}$ and the parameters a and ϕ are presented for four considered in this paper high symmetry directions of the wave vector in the limit $\boldsymbol{k} \to \boldsymbol{0}$. The relations for other directions of $\boldsymbol{k}$ and the explanation how they were calculated can be found in [15].

TABLE

Hole spin projections $\{\langle J_x \rangle, \langle J_y \rangle, \langle J_z \rangle\}$ for heavy-mass, light-mass, and split-off bands for high symmetry directions of the wave vector $\boldsymbol{k}$ considered in this paper. $S = 2a\sqrt{1-a^2}\sin\phi$, $C = 2a\sqrt{1-a^2}\cos\phi$, $Q = 1 - 2a^2$. The quantization axis is parallel to z direction.

$\boldsymbol{k}$	Heavy-mass band	Light-mass band	Split-off band
[001]	$\{0, 0, -\frac{3}{2}Q\}$	$\{C, S, -\frac{1}{2}Q\}$	$-\frac{1}{2}\{C, S, Q\}$
[010]	$\{-\frac{3}{2}C, 0, 0\}$	$\{-\frac{1}{2}C, S, Q\}$	$-\frac{1}{2}\{C, S, Q\}$
[111]	$\frac{1}{6}(C + S - 5Q)$	$\frac{1}{6}\{-C + 5S + Q, -5C$	$\frac{1}{6}\{2C - S + 2Q, C - 2S$
	$\times\{1, -1, 1\}$	$+S - Q, -C - S - 5Q\}$	$-2Q, -2C - 2S + Q\}$
[1$\bar{1}$1]	$\frac{1}{6}(C - S + 5Q)$	$\frac{1}{6}\{-C - 5S - Q, 5C$	$\frac{1}{6}\{2C + S - 2Q, -C - 2S$
	$\times\{1, 1, -1\}$	$+S - Q, C - S - 5Q\}$	$-2Q, 2C - 2S + Q\}$

The following observations related to Table will be noted. In general, for a given $\boldsymbol{k}$ the spin $\langle \boldsymbol{J} \rangle$ may point in any direction, however, its length depends on the angle between $\boldsymbol{k}$ and $\langle \boldsymbol{J} \rangle$. The end of $\langle \boldsymbol{J} \rangle$ spans a closed surface when a and ϕ is varied, respectively, in the range $a = (0 \ldots 1)$ and $\phi = (0 \ldots 2\pi)$. For heavy-mass holes, when $\boldsymbol{k}$ is parallel to one of high symmetry crystallographic axes, the spin surface reduces to a line. For example, as seen from Table, if the heavy-mass hole is propagating in y direction, i.e. along [010] crystallographic axes, then its average spin will be along x axis and the magnitude of it will lie in the range from $-\frac{3}{2}$ to $+\frac{3}{2}$. If the hole is in the split-off band, then the average spin surface is the sphere of radius $|\langle \boldsymbol{J} \rangle| = \frac{1}{2}$, since $\sqrt{(-\frac{1}{2})^2(Q^2+S^2+C^2)} = \frac{1}{2}$, where Q, S, and C are defined in Table. In case of light-mass hole the spin surface is an ellipsoid. The surfaces that belong to the family of wave vectors of the same symmetry are related by symmetry relations of the corresponding wave vector star. If the hole is propagating along lower symmetry direction, say, along [111] crystallographic axes, the heavy-mass hole spin will be parallel to $[1\bar{1}1]$ direction and will range from $-\frac{5\sqrt{3}}{6}$ to $\frac{5\sqrt{3}}{6}$. However, for this direction, as follows from Table, the light-mass and split-off hole spins are characterized by more general second-order surfaces.

At finite $\boldsymbol{k}$'s, one must use numerical methods to find the relation between the parameters a and ϕ and the average spin $\langle \boldsymbol{J} \rangle$. Examples can be found in Ref. [15]. Figure 1 and similar figures in [15] for GaAs and InP may serve as a guide, when $\boldsymbol{k} = \boldsymbol{0}$ approximation breaks down. From what has been said the remarkable point to be noted is that the parameters a and ϕ relate the properties of the ballistically injected spin into degenerate bands with those of the initial wave function in the Schrödinger equation.

The spin dynamics and intervalence transitions were described by the following Schrödinger system of equations for the six-component state-vector $|\psi\rangle$ in the effective mass approximation

$$\mathrm{i}\hbar \frac{\partial |\psi\rangle}{\partial t} = [H_{\mathrm{LK}}(\boldsymbol{k}) + H_{\mathrm{F}}(\boldsymbol{k})]\,|\psi\rangle, \tag{2}$$

where $\mathrm{i} = \sqrt{-1}$ and $\hbar$ is the Planck constant. $H_{\mathrm{LK}}(\boldsymbol{k})$ is the 6×6 Luttinger–Kohn Hamiltonian [17, 18], which is a function of the hole wave vector $\boldsymbol{k} = (k_x, k_y, k_z)$. $H_{\mathrm{F}}(\boldsymbol{k})$ is the field term. Using the equation of motion for the wave vector

$$\mathrm{d}\boldsymbol{k}/\mathrm{d}t = (e/\hbar)\boldsymbol{F}(t) \tag{3}$$

in the electric field $\boldsymbol{F}$, the Schrödinger system (2) can be transformed from partial to total derivatives. The correct form of the field Hamiltonian $H_{\mathrm{F}}(\boldsymbol{k})$ was derived recently in [19], where it was shown that the $H_{\mathrm{F}}(\boldsymbol{k})$, along with the term that is proportional to electric field F_j, must also include the terms proportional to $k_i F_j$ and F_j^3, where $i, j = x, y, z$. In the following only the leading term proportional to the electric field was retained:

$$H_{\mathrm{F}}(\boldsymbol{k}) \approx \frac{e\boldsymbol{F}(t)}{\mathrm{i}} \frac{\partial}{\partial \boldsymbol{k}}, \tag{4}$$

where e is the elementary charge. Estimation of the higher order terms in $H_{\rm F}(\boldsymbol{k})$ shows that their contribution does not change qualitatively the results presented below.

The time dependence of the average spin projections was found from

$$\langle J_j \rangle_i = \langle \psi_i | J_j | \psi_i \rangle, \tag{5}$$

where J_j is j-th component of the total 6×6 angular momentum matrix. The subscript j denotes the Cartesian component (x, y, or z) and the subscript i denotes the band (i = h, l, or s). The concrete forms of the matrices J_j can be found in [15]. The numerical singular value decomposition was used to connect the state vector $|\psi\rangle$ in spinor representation and its partner in the energy band representation, for example, represented by expression (1).

3. Stepped and harmonic field

In this and next section numerical results on spin evolution of the valence hole in constant and time-varying electric fields is presented. In all figures the ballistic hole, at the moment $t = 0$, is assumed to be injected in the heavy-mass band and possess the wave function (1). Silicon valence band parameters were used in the simulation.

Figure 2 shows hole spin precession induced by stepped electric field of the amplitude 20 kV/cm. In Fig. 2a the electric field $\boldsymbol{F}$ is parallel to [100] direction and at the same time is perpendicular to the wave vector $\boldsymbol{k} = (k_{x0}, k_{y0}, k_{z0}) = (0, 0, 0.472)$ nm^{-1}. The initial spin was maximized in accordance with Table. The initial energy of the hole is $\varepsilon_{\rm h0} = 26.86$ meV. In Fig. 2b, $\boldsymbol{F} \parallel [111]$ and $\boldsymbol{k} = 0.109 \times (1, -1, 1)$ nm^{-1}. The precession of the spin may be understood by noting that, according to Eq. (3), the wave vector is proportional to time and that the strongest mixing of the heavy- and light-mass bands due to electric field occurs when the wave vector is close to the Brillouin zone center. The mixing of the wave

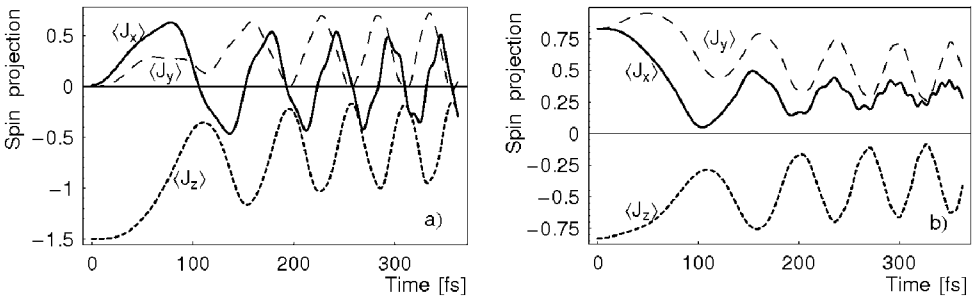

Fig. 2. Precession of the hole spin induced by 20 kV/cm field step switched on at the moment $t = 0$. (a) $\boldsymbol{F} \parallel [100]$, $\boldsymbol{k}_0 \parallel [001]$, (b) $\boldsymbol{F} \parallel [111]$, $\boldsymbol{k}_0 \parallel [1\bar{1}1]$.

functions results in hole tunneling to the light-mass band and subsequent beating between heavy- and light-mass band wave functions. The beating amplitude is the largest when in the superposition state the contribution of both bands is of a comparable magnitude. When the hole is far away from the Brillouin zone center the mixing of the wave function by electric field ceases, however, the average energy of the hole in the superposition states continues to grow. As a result the beating frequency between heavy- and light-mass bands grows, which is also reflected in the spin precession frequency, too.

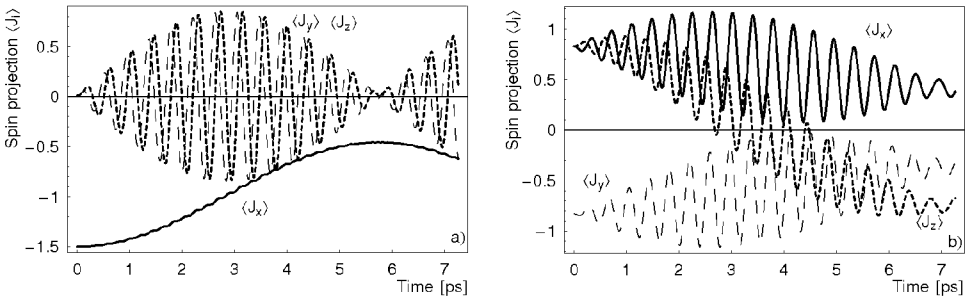

Fig. 3. Evolution of spin components in harmonic and linearly-polarized field at resonance, when $\boldsymbol{F} \parallel [001]$. The initial wave vector and field amplitude: (a) $\boldsymbol{k}_0 = (0, 0.3778, 0)\ \mathrm{nm}^{-1}$, $F_0 = 617$ V/cm; (b) $\boldsymbol{k}_0 = 0.1417 \times (1, 1, 1)\ \mathrm{nm}^{-1}$, $F_0 = 1440$ V/cm.

Figure 3 shows the evolution of spin components under harmonic excitation. The frequency ω of the field was tuned to heavy-light transition: $\hbar\omega = 9.81$ meV in Fig. 3a and $\hbar\omega = 10.78$ meV in Fig. 3b. The initial spins are different in both figures. Two types of oscillations, fast and slow, are clearly seen. The slow ones are associated with the Rabi oscillation of hole population between heavy- and light-mass bands. The period of the Rabi oscillations is proportional to field amplitude F_0. In Fig. 3a, the change of the band population correlates with the change of $\langle J_x \rangle$ component between $-\frac{3}{2}$ and $-\frac{1}{2}$. The maximum of $\langle J_x \rangle$ corresponds to total hole transfer from the heavy- to light-mass band. The frequency of the fast oscillations, which are the most clearly seen in $\langle J_y \rangle$ and $\langle J_z \rangle$ components in Fig. 3a, coincides with the exciting field frequency ω. If ω is chosen to be slightly out of the resonance, then an additional beating between the resonance and laser frequencies, similarly as it is observed in the atomic transitions, occurs. The main difference between Fig. 3a and b is that in the former the initial and final spin points in the same direction, while in the latter the initial and final spin points in different directions. Also, the change of the magnitude of the spin in Fig. 3a is larger than in b. This reflects the general property of the spin–orbit interaction: it is proportional to the mixed vectorial product $\boldsymbol{J} \cdot (\boldsymbol{F} \times \boldsymbol{k})$. As a result it is the strongest when the vectors $\boldsymbol{J}$, $\boldsymbol{F}$, and $\boldsymbol{k}$ are mutually orthogonal, as in Fig. 3a. By the same reason, if the two of three vectors are parallel, the intervalence transitions are forbidden and, consequently, the population and spin do not change with time.

Figure 4 shows the case, where circularly polarized field is used to induce heavy-light transitions. The field vector is rotating in the k_x-k_z plane, while the initial hole wave vector is perpendicular to k_x-k_z plane. Figure 4a and b corresponds, respectively, to spin initially pointing in one of two opposite directions, or equivalently they correspond to right- and left-handed polarization of the field. The inversion of the spin was achieved by tuning a and ϕ values in the initial spinor (1). When the field is rotating clockwise, Fig. 4a, the spin change is the strongest. It corresponds to the selection rule $\Delta J = 1$. The transition rate is twice larger than that for linearly polarized light at the same field amplitude. If spin or polarization is reversed to opposite, Fig. 4b, the transition, in accordance with

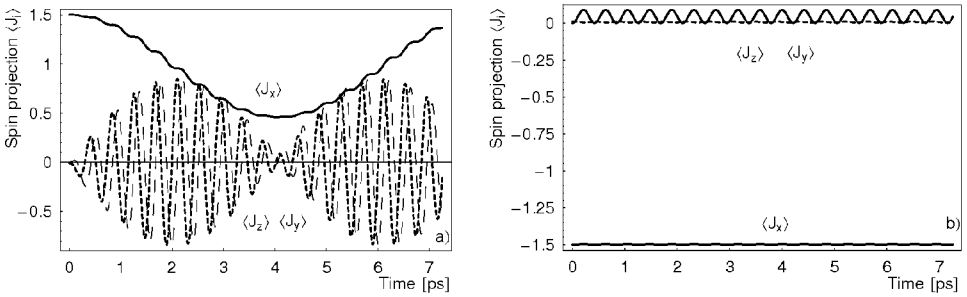

Fig. 4. Evolution of the spin components in the resonant harmonic and circularly-polarized electric field. The initial wave vector and field amplitude: $\boldsymbol{k}_0 = (0, 0.3778, 0)$ nm^{-1}, $F_0 = 436$ V/cm. Parts (a) and (b) correspond to opposite directions of the initial spin.

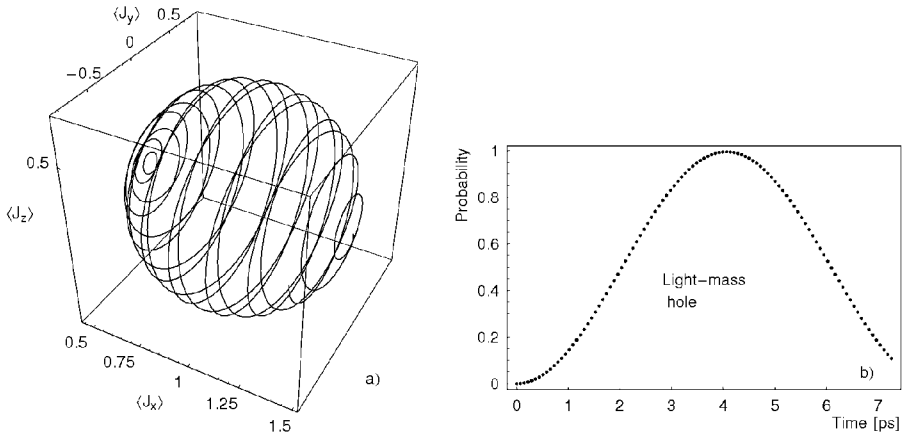

Fig. 5. (a) Hole spin trajectory in 3D spin space for right-handed polarization. (b) Corresponding dependence on time of the probability to find the hole in the light-mass band.

the selection rules, is forbidden. A small ripple seen in Fig. 4b is due to harmonic motion of $\boldsymbol{k}$ that is synchronous with the exciting field. The spin selection rules seen in the two parts of Fig. 4 are also mirrored in the time-dependence of the hole population: it was observed that the probability for a hole to be in the light-mass band oscillated between 0 and 1 with the same Rabi frequency for allowed transitions and practically did not change when the initial polarization was reversed to opposite. In Fig. 5a, the curves from Fig. 4a are replotted parametrically in three dimensions. As can be seen the end-point of the spin vector at first spirals out and then returns back to its initial position in a slightly different trajectory. The difference is associated with a small shift from the exact resonance (the Bloch–Siegert shift). For comparison, Fig. 5b shows the time-dependence to find the hole in the light-mass band for this case.

4. Optimized fields

The quantum control is based on the coherent evolution of the quantum system and manipulation of the coherence [20]. For this purpose specially tailored external fields are used which, for example, maximize the probability to achieve the desired target state or which excite the target-level as fast as possible for a fixed exciting pulse energy. Earlier it was shown that in case of interband transitions the shape of the exciting pulse is not unique [21]. In the semiconductor spintronics, similarly, it would be interesting to know how to achieve spin flipping as fast as possible by manipulating the spin states with pulses of finite or minimal energy. To optimize the transition rate between two spin states the controlling electric field was approximated by the formula

$$F(t) = F_0 \sin[\omega t + \alpha(t - t_\mathrm{d})^2 + \varphi] \exp\left(-\sum_{n=1}^{4} a_n \tau^n\right), \tag{6}$$

where $\tau = (t - t_\mathrm{d})/t_\mathrm{f}$. Here, t_f is the final simulation time and t_d is the delay time. The relation $t_\mathrm{d} = t_\mathrm{f}/2$ was used. In Eq. (6) eight parameters — amplitude F_0, angular frequency ω, chirping coefficient α, initial phase φ, and four parameters a_n which determine the envelope shape of the field — were varied to achieve an optimal transition.

Figure 6 shows an optimal pulse selected by varying parameters in Eq. (6) "by hand" and Fig. 7a shows the resulting evolution of the hole spin projections. The initial wave vector is (0,0.425,0) nm^{-1} and the electric field is linearly polarized in the z direction. The optimization was performed with $\langle J_x \rangle$ component only. It is interesting that the femtosecond switching of $\langle J_x \rangle$ from $-\frac{3}{2}$ to $-\frac{1}{2}$ state is accompanied by simultaneous excitation and subsequent decay of the other two spin projections. In three dimensions this yields a spiral-like trajectory similar to that seen in Fig. 5a. It was observed that after termination of the pulse the spin was precessing about some axis if the energy of the pulse and its shape were not optimal

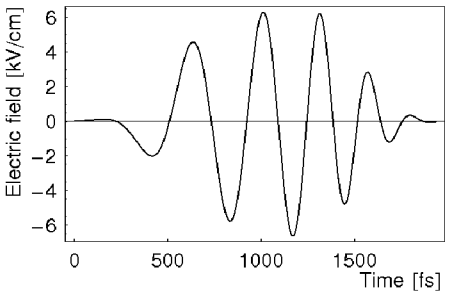

Fig. 6. Shape of the electric field $F_z(t)$ optimized to $\langle J_x \rangle$ transition from $-\frac{3}{2}$ to $-\frac{1}{2}$ state.

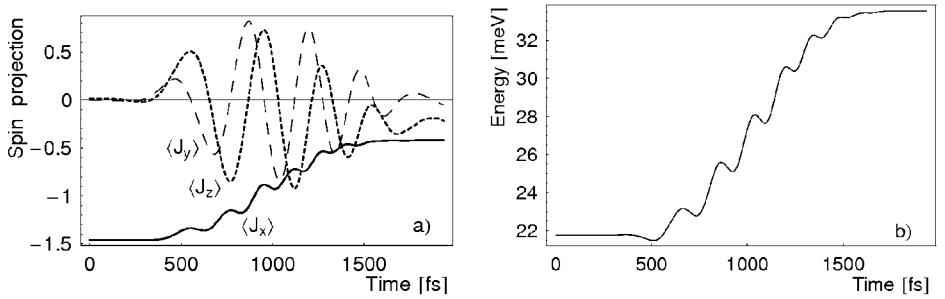

Fig. 7. Evolution of spin projections (a) and average energy (b) under excitation of the heavy hole by electric pulse shown in Fig. 6.

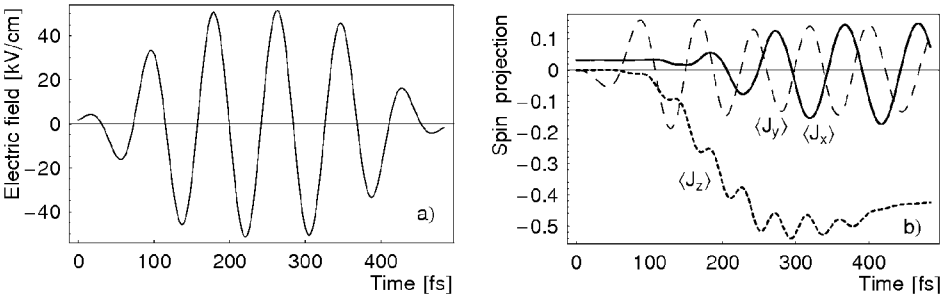

Fig. 8. Electric field $F_z(t)$ optimized to heavy–split-off band transition (a) and the evolution of the hole spin projections (b). $\boldsymbol{k}_0 = (0, 0.378, 0)$ nm^{-1}.

(cf. Fig. 8b). As known, during procession the end of the vector $\langle \boldsymbol{J} \rangle$ runs round the circle in three dimensions in case of simple spin systems. However, for warped and parabolic bands the precession trajectory may have an additional small chaotic component on the circle. It was found that the spin-optimized femtosecond pulse at the same time was the π-pulse, since such pulse also excited light-mass band with the probability equal to one. For comparison, Fig. 7b shows time dependence of the average energy. The initial and final energies correspond, respectively, to heavy- and light-mass band values.

Up till now in the simulation the average exciting photon energy was smaller than the optical phonon energy. Since the characteristic optical phonon emission time is short, about one picosecond, for larger photon energies, for example when the split-off band is excited too, the theory should be generalized to include the dissipation [13]. Nonetheless, for completeness, in Fig. 8 the coherent excitation from heavy-mass to split-off band is shown to illustrate that in principle one can control spin for these transitions as well. We should note that in this case the parameters a and ϕ were chosen so as to make the initial spin close to zero.

5. Conclusions

The paper shows that in bulk semiconductors the initial spin of the hole (its direction and the magnitude) can be described by two parameters a and ϕ that appear in the wave function of the heavy-mass, light-mass, or split-off valence subbands. This feature allows one to link the observables, such as spin projections, with the initial wave function of the time-dependent Schrödinger equation. In general case, when bands are nonspherical and nonparabolic, the parameters a and ϕ are to be precalculated from the corresponding stationary Schrödinger equation. For small wave vectors, analytical relations between spin properties and parameters a and ϕ for some high symmetry directions can be used as shown in Table.

Simulation of the hole intervalence dynamics in high electric fields, when intervalence hole tunneling prevails, shows that, in principle, it is possible to manipulate with spin degrees of freedom of the ballistically moving hole. Simulation also shows that the spin switching and the hole intervalence population changes are intimately related, although the optimization of one does not necessarily implies the optimization of the other. It was shown that in bulk p-type semiconductors it is possible to transfer the hole spin coherently between two spin states in times shorter than hole collision time with the optical phonons.

The optimized electrical pulses in Figs. 6 and 8 consist of about 4 or 8 optical periods. The experiments with phase-matched difference–frequency mixing in GaSe [22] show that it is feasible to generate such ultrashort pulses at the output energies as high as 1 μJ in the mid-infrared spectral range. The electric field of such pulses is high enough to excite coherent intervalence transitions. Theoretical study of the optimal interband population excitation in Ref. [21] shows that the exciting pulses may be even shorter, up to a half of the optical period, and that the largest population inversion rate is bounded by a fundamental limitation related to time-energy uncertainty. Since the spin switching and the transfer of the hole population between energy bands as shown in this paper are interrelated, the maximum spin switching rate is expected to be limited by the time-energy uncertainty relation too.

References

[1] The status of spintronics is fully reflected in the "Proceedings of the PASPS Conference", *J. Superconductivity: Incorporating Novel Magnetism* **16**, No. 1 and No. 2 (2003).

[2] R.R. Ernst, G. Bodenhausen, A. Wokaun, *Principles of Nuclear Magnetic Resonance in One and Two Dimensions*, Clarendon Press, Oxford 1987.

[3] J. Kessler, *Polarized Electrons*, Springer-Verlag, Berlin 1985.

[4] J. Kessler, *Can. J. Phys.* **74,** 863 (1996).

[5] *Modern Problems in Condensed Matter Sciences, Optical Orientation*, Eds. F. Meier, B.P. Zakharchenya, Vol. 8, North-Holland, Amsterdam 1984.

[6] S. Datta, B. Das, *Appl. Phys. Lett.* **56,** 665 (1990).

[7] X. Cartoixà, D.Z.-Y. Ting, Y.-C. Chang, *Appl. Phys. Lett.* **83,** 1462 (2003).

[8] V.Ya. Aleshkin, Yu.A. Romanov, *Zh. Eksp. Teor. Fiz.* **87,** 1857 (1984).

[9] A. Dargys, A.F. Rudolph, *Phys. Status Solidi B* **135,** 437 (1986).

[10] A. Dargys, A.F. Rudolph, *Phys. Status Solidi B* **140,** 535 (1987).

[11] C. Jacoboni, L. Reggiani, *Rev. Mod. Phys.* **55,** 645 (1987).

[12] A. Dargys, *Phys. Rev. B* **66,** 165216 (2002).

[13] A. Dargys, *Phys. Scr.* **67,** 505 (2003).

[14] A. Dargys, P. Harrison, *Semicond. Sci. Technol.* **18,** 247 (2003).

[15] A. Dargys, *Phys. Status Solidi B* **241,** 145 (2004).

[16] Y. Ohno, D.K. Young, B. Beschoten, F. Matsukura, H. Ohno, D.D. Awschalom, *Nature* **402,** 790 (1999).

[17] J.M. Luttinger, W. Kohn, *Phys. Rev.* **97,** 869 (1955).

[18] G.L. Bir, G.E. Pikus, *Symmetry and Strain-Induced Effects in Semiconductors*, Wiley, New York 1974.

[19] A. Foreman, *J. Phys., Condens. Matter* **12,** R435 (2000).

[20] I. Walmsley, H. Rabitz, *Phys. Today* **56,** 43 (2003).

[21] A. Dargys, *Phys. Rev. B* **64,** 235123 (2001).

[22] R.A. Kaindl, M. Wurm, K. Reimann, P. Hamm, A.M. Weiner, M. Woerner, *J. Opt. Soc. Am. B* **17,** 2086 (2000).